Texture Analysis Using Gaussian Weighted Grey Level Co-occurrence Probabilities

Rishi Jobanputra, David A. Clausi
University of Waterloo, Waterloo, Ontario, N2L 3G1
rjobanpu@uwaterloo.ca

***Abstract*— The discrimination of textures is a significant aspect in segmenting SAR sea ice imagery. Texture features calculated from grey level co-occurring probabilities (GLCP) are well accepted and applied in the analysis of many images. When calculating GLCPs, each co-occurring pixel pair within the image window is given a uniform weighting. Although a novel technique, co-occurring texture features have a tendency to misclassify and erode texture boundaries due to the large window sizes needed to capture meaningful statistics.**

A method is proposed whereby co-occurring pixel pairs closer to the center of the image window are assigned larger co-occurring probabilities according to a Gaussian distribution. By using a Gaussian weighting scheme to calculate the GLCPs, less significance is given to pixel pairs that are on the outlying regions of the window, which have a tendency to produce erroneous statistics as the image window overlaps a texture boundary. This method proves to preserve the edge strength between textures and provides better segmentation at the expense of computational complexity.

***Index Terms*— Grey level co-occurrence probabilities; texture analysis; image segmentation; SAR sea ice; texture features; remote sensing imagery**

I. Introduction

THE use of synthetic aperture radar (SAR) to monitor sea ice is becoming extremely popular to due its accessibility and accuracy. Providing images that discriminate pertinent ice types is important for operational communities (e.g. ships, oil platforms, etc) and monitoring climatic changes (e.g. global warming). Although easily segmented by the human observer, there is no robust automated machine approach that can separate relevant ice types from an image.

Automated computer interpretation of SAR sea ice imagery is exceedingly challenging because of varying imaging parameters, environmental factors, platform resolution, and electromagnetic properties of active sensors (i.e. speckle noise). These aspects can create inconsistencies in the tone and texture of the SAR sea ice appearance and make it difficult to formulate a robust automated segmentation algorithm.

In general, unsupervised image segmentation involves (1) extracting each pixel's features and (2) clustering together like pixels based their features. Extracting properties of texture from images make excellent features for segmenting SAR data. Texture features can be categorized as statistical, structural, signal-based and model-based (Tuceryan & Jain 1993). This paper intends on investigating statistical-based features generated by grey level co-occurring probabilities (GLCP), developed Haralick et al. (1973), which have been extensively used in feature extraction of remote sensing imagery.

A drawback of using co-occurring textures for SAR sea ice segmentation is that they have a tendency to misclassify and erode texture boundaries, especially for large window sizes and irregular texture boundaries (Clausi & Yue 2003). Although large window sizes will erode texture boundaries, they are necessary to gather sufficient data to characterize local texture regions; small window sizes will result in poorly sampled GLCPs, which produce incoherent statistics.

In this paper, a Gaussian weighting scheme is proposed for calculating the co-occurring probabilities whereby pixel pairs closer to the center of the image window are given a higher probability than those on the outlying edges. This paper intends on comparing the texture features generated by weighted grey level co-occurring probabilities (WGLCP) to the GLCP features with respect to their boundary preservation and segmentation ability.

This paper is arranged in the following manner. In Section II, a derivation of the grey level co-occurrence method is given. A complete formulation of the WGLCP texture features and implementation details are described in Section III. Section IV provides a comparison of the GLCP and WGLCP texture features and their discriminating abilities while the final Section (V) summarizes and concludes the paper.

II. Grey Level co-occurrence texture features

The GLCPs provide a second-order method for generating texture features (Haralick et al. 1973). Given a spatial window within the image, the GLCPs represent the conditional joint probabilities of all pair-wise combinations of grey levels given two parameters: interpixel distance (δ) and orientation (θ). It should be noted that since the image window is a discrete set, it is convenient to represent the parameters δ and θ as Cartesian co-ordinates δ_x and δ_y which represent the interpixel spacings in the x- and y-directions respectively. The probability measure can be defined as:

$$Pr(x) = \{C_{ij} \mid (\delta_x, \delta_y)\} \tag{1}$$

where C_{ij} (the co-occurrence probability between grey levels i and j) is defined as:

$$C_{ij} = \frac{P_{ij}}{\sum_{i,j=1}^{G} P_{ij}} \tag{2}$$

where P_{ij} represents the frequency of occurrence betwe grey levels, *i* and *j*, for a given displacement vector (

Proceedings of the First Canadian Conference on Computer and Robot Vision (CRV'04)
0-7695-2127-4/04 $20.00 © 2004 IEEE

TABLE I

GREY LEVEL SHIFT-INVARIANT CO-OCCURRENCE TEXTURE STATISTICS

Maximum probability (MAX)	$max(C_{ij})$ for all (i,j)
Uniformity (UNI)	$\sum C_{ij}^2$
Entropy (ENT)	$\sum C_{ij} log C_{ij}$
Dissimilarity (DIS)	$\sum C_{ij}\|i-j\|$
Contrast (CON)	$\sum C_{ij}(i-j)^2$
Inverse difference (INV)	$\sum \frac{C_{ij}}{1+\|i-j\|}$
Inverse difference moment (IDM)	$\sum \frac{C_{ij}}{1+(i-j)^2}$
Correlation (COR)	$\sum \frac{(i-\mu_x)(j-\mu_y)C_{ij}}{\sigma_x \sigma_y}$

for the specified window size. G is the number of quantized grey levels for the entire image. The sum in the denominator represents the total possible number of grey level pairs (i,j) within the window, given (δ_x, δ_y).

Statistics are applied to the GLCPs to generate texture features. Although many texture statistics can be applied, eight common grey level shift invariant statistics are considered (Table I). From the literature (Baraldi & Parmiggiani 1995), it has been determined that statistics which are grey level shift invariant are best suited for SAR imagery so that classification is not a function of tone.

Historically, the GLCPs are stored inefficiently in a $G \times G$ sparse matrix known as the grey level co-occurrence matrix (GLCM). When using GLCMs, the fewer number of grey levels, G, the faster the computation of the features. There have been advances in the computation time required to calculate the co-occurring statistics through the use of grey level co-occurring linked lists (GLCLL) (Clausi & Jernigan 1998), or the grey level co-occurrence hybrid structure (GLCHS) (Clausi & Zhao 2002). In contrast to the GLCM technique, these methods avoid storing zero probabilities for grey level pairs.

III. FORMULATION OF THE WEIGHTED CO-OCCURRENCE TEXTURE FEATURES

When calculating traditional co-occurring texture features, all the co-occurring pixel pairs within the image window are considered to have a uniform probability. To improve on the texture features for the purposes of segmentation, pixel pairs closer to the center of the image window should be given higher significance than those on the border. As illustrated in Figure 1, the location of the pixel pair to the center of the image window determines the relative frequency of co-occurrence.

Assume the effective image window, W, is rectangular with n_x columns and n_y rows (where n_x and n_y are odd numbers). Then the image window can be indexed as follows:

$$W_x \quad \epsilon \quad \left\{ -\lfloor \frac{n_x}{2} \rfloor, -(\lfloor \frac{n_x}{2} \rfloor - 1), \ldots, (\lfloor \frac{n_x}{2} \rfloor - 1), \lfloor \frac{n_x}{2} \rfloor \right\}$$

$$W_y \quad \epsilon \quad \left\{ -\lfloor \frac{n_y}{2} \rfloor, -(\lfloor \frac{n_y}{2} \rfloor - 1), \ldots, (\lfloor \frac{n_y}{2} \rfloor - 1), \lfloor \frac{n_y}{2} \rfloor \right\}$$

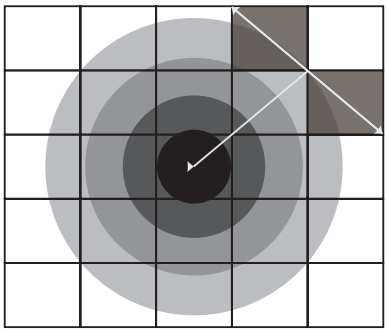

Fig. 1. Measuring the pixel pair distance to the center of the image window

(3)

where $W_x \times W_y$ is the set of pixels in the image window indexed by their x-y (i.e. column-row) designations as outlined by the example in Table II. This indexing scheme was chosen so that center pixel in the image window will have an index of $(0,0)$ which is convenient for calculating the WGLCPs. The grey levels in the image window can be represented as a function of the index as follows:

$$W(x,y) = i, \ where \ i \subseteq \{0, 1, \ldots G-1\} \tag{4}$$

Given two pixels in the image window that are separated by (δ_x, δ_y), one with grey level i, the other with grey level j, the point that bisects the line connecting $W(x_1, y_1)$ and $W(x_2, y_2)$ is defined as follows:

$$\begin{aligned} r_{ij} &= r_{ij}(W(x_1,y_1), W(x_2,y_2)) \\ &= \left(\frac{x_1+x_2}{2}, \frac{y_1+y_2}{2} \right) \\ &= (r_x, r_y) \\ &\quad \Big| W(x_1,y_1) = i, W(x_2,y_2) = j \\ &\quad (\delta_x, \delta_y) = (x_1 - x_2, y_1 - y_2) \end{aligned} \tag{5}$$

Previously in Equation 2, P_{ij} was defined as the frequency of co-occurrence between two grey levels. However, in this formulation, P_{ij} is the weighted co-occurring frequency and is a Gaussian function of r_{ij}. Formally, for a fixed interpixel

TABLE II

THE IMAGE WINDOW ($W_x \times W_y$) INDEXING SCHEME

W(-2,-2)	W(-1,-2)	W(0,-2)	W(1,-2)	W(2,-2)
W(-2,-1)	W(-1,-1)	W(0,-1)	W(1,-1)	W(2,-1)
W(-2,0)	W(-1,0)	W(0,0)	W(1,0)	W(2,0)
W(-2,1)	W(-1,1)	W(0,1)	W(1,1)	W(2,1)
W(-2,2)	W(-1,2)	W(0,2)	W(1,2)	W(2,2)

Proceedings of the First Canadian Conference on Computer and Robot Vision (CRV'04)
0-7695-2127-4/04 $20.00 © 2004 IEEE

displacement vector (δ_x, δ_y), the weighted co-occurring frequencies are as follows:

$$P_{ij} = \sum_{\forall r_{ij}} \frac{1}{2\pi\sigma_x\sigma_y} \exp\left\{ -\frac{1}{2}\left[\left(\frac{r_x}{\sigma_x}\right)^2 + \left(\frac{r_y}{\sigma_y}\right)^2\right]\right\} \tag{6}$$

where σ_x and σ_y represent the standard deviation of the Gaussian pdf in the x- and y-directions respectively. Using Equation 2, the frequencies are normalized to produce the probability measures.

To maximize the energy of the Gaussian pdf within the effective image window, the standard deviations are selected to be $\frac{1}{5}$ of the window size. This captures approximately 90 percent of the pdf's energy (area) in the effective window. Formally, the window size can be written as a function of the standard deviation as follows:

$$n_x = \begin{cases} 5\sigma_x & \text{if } 5\sigma_x \text{ is odd} \\ 5\sigma_x + 1 & \text{if } 5\sigma_x \text{ is even} \end{cases}$$

$$n_y = \begin{cases} 5\sigma_y & \text{if } 5\sigma_y \text{ is odd} \\ 5\sigma_y + 1 & \text{if } 5\sigma_y \text{ is even} \end{cases} \tag{7}$$

In the current implementation, the WGLCPs are stored in a $G \times G$ matrix similar to the GLCM. Once the WGLCPs have been normalized, the texture statistics (Table I) can be applied.

IV. Analysis and Comparison

A. Objectives

The purpose of this study is to investigate and compare the texture features generated from WGLCPs and GLCPs. Three tests are performed for determining the preferred feature set: (1) segmentation ability, (2) texture boundary edge strength and (3) computational speed.

B. Parameters

There are a number of parameters required for the calculation of GLCP and WGLCP texture features. First, the quantization of the image grey levels reduces the memory and computational demands. Typically, the image is quantized from an 8 bit (256 levels) representation to 4 or 5 bits. As outlined in the literature (Clausi 2002), a 5 bit (32 levels) representation of the image is preferred when calculating co-occurring features. Secondly, it is ideal to have a minimal number of texture features by minimizing the number of parameters used (distances, orientations, statistics). The interpixel displacement vectors selected are dependent on the nature and resolution of the textures to be segmented. For most SAR sea ice imagery, the interpixel spacing is selected for four orientations $(0°, 45°, 90°, 135°)$ with a displacement of 1. It is recommended (Barber & LeDrew 1991) that only three statistics be used. Studies have shown that *entropy, contrast and correlation* form an appropriate set of statistics (Soh & Tsatsoulis 1999). Third, the window size must be large enough to characterize the region of interest but remain sufficiently small as to not erode texture boundaries. As well, the resolution of the image is a factor when determining window size. Research indicates that a window size of 15×15 is preferred for SAR sea ice imagery (Barber et al. 1993) for most satellite platforms. Table III summarizes the GLCP and WGLCP parameters used for this study.

TABLE III
GLCP and WGLCP Parameters Used

GLCM	PARAMETERS	WGLCM
(1,0), (1,1), (0,1), (-1,1)	**Displacement Vector**	(1,0), (1,1), (0,1), (-1,1)
32 levels	**Quantization**	32 levels
ent, con, cor	**Statistics**	ent, con, cor
15×15	**Window Size**	15×15
n/a	**Standard Deviation**	3

C. Image data sets

To address the segmentation abilities of the GLCP and WGLCP features, two texture image sources are studied. Test Set 1 (Figure 2) is a SAR sea ice image of the Beaufort area taken from the RADARSAT-I platform with a nominal resolution of 150 m with 100 m pixel spacing. A manual segmentation of the image is included with the test set and is used as *ground truth* for analysis.

Test Set 2 (Figure 4) is RADARSAT-I SAR imagery of the Baffin Bay area. The nominal resolution is 150 m with 100 m pixel spacing. As above, the manual segmentation of the image is included in the test set and will be used in analysis. This image was selected due to the numerous amount of cracks within the ice floes. These cracks increase the number of ice-water boundaries in the image and prove to be very challenging for segmentation.

D. Segmentation Ability

Using the parameters in Table III, the GLCP and WGLCP texture features were calculated and scaled using linear normalization for all test sets. The features were scaled to improve segmentation by providing a consistent resolution along all dimensions of the features space. From these feature sets, K-means clustering was applied. Figures 3 and 5 show the segmentation results of K-means clustering for the SAR images of the Beaufort and Baffin regions respectively. For both images, the manually segmented boundaries are overlayed (in grey) to provide a better indication of the segmentation results.

By viewing the lower right quadrant of the segmented Beaufort images (Figure 3), it is apparent that the WGLCP features perform better at segmenting regions close to boundaries. In general, there are fewer pixels incorrectly classified as water near boundary regions; this is reflected by a 15 % increase producers's accuracy for water when using the WGLCP [illegible] features. Table IV lists all the accuracies for the Be[illegible]

Proceedings of the First Canadian Conference on Computer and Robot Vision (CRV'04)
0-7695-2127-4/04 $20.00 © 2004 IEEE

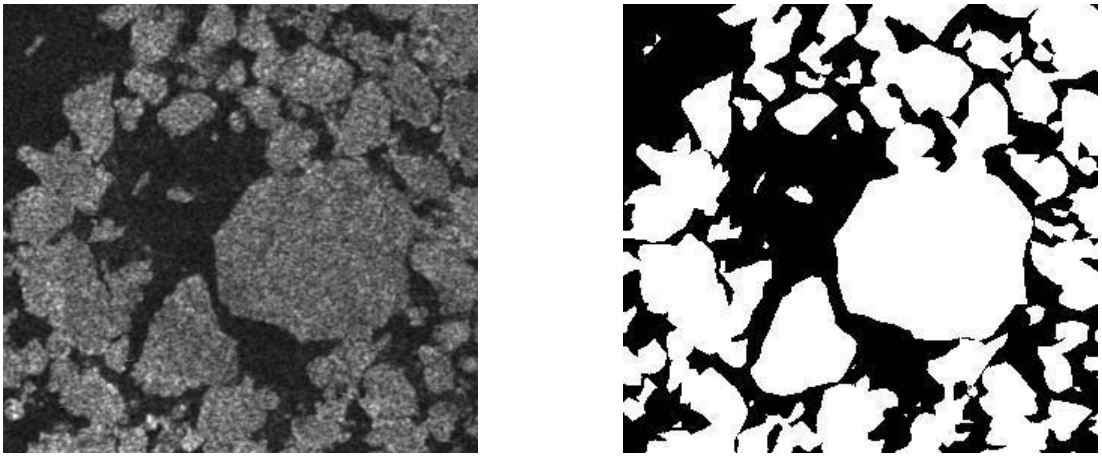

(a) Original (b) Manual Segmentation

Fig. 2. Test Set 1: SAR Sea Ice Image from Beaufort Bay

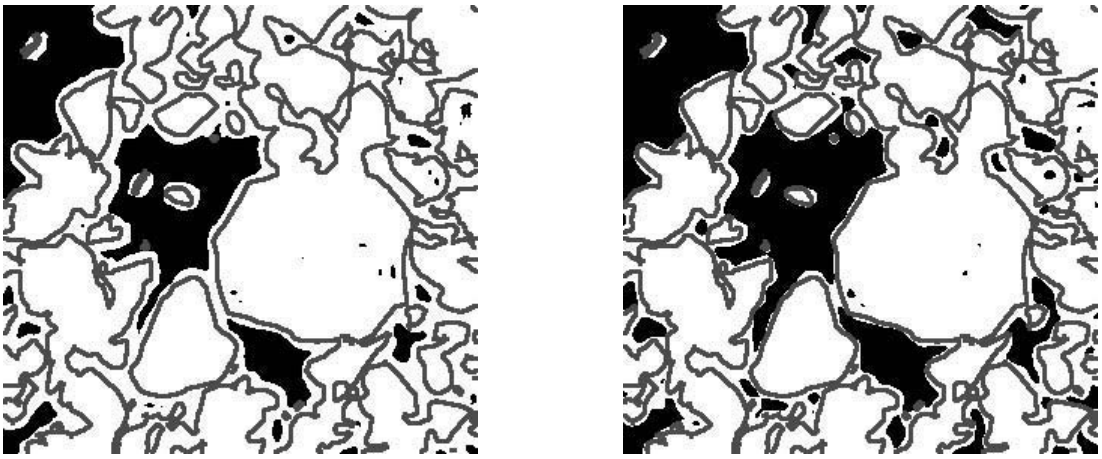

(a) Segmentation using GLCP feature set (b) Segmentation using WGLCP feature set

Fig. 3. Segmentation Results from Test Set 1: SAR Sea Ice Image from Beaufort Bay

Image (Test Set 1) and indicates that there was a 6 % increase in the overall accuracy for the WGLCP feature set.

The segmented Baffin images (Figure 5) also display the same behaviors as Test Set 1. In general, WGLCP texture features perform better at segmenting regions close to boundaries. Formally, Table V indicates that there was a 3 % increase in the overall accuracy when using the WGLCP features. Although there was an increase in accuracy for the WGLCP features, both algorithms were unable to detect the cracks in the lower portion of the image. This is a result of the window size being too large.

For both test sets, there was a significant increase in the user's accuracy for ice classification and the producer's accuracy for water classification. Both of these statistics are positively correlated and indicate that more ice pixels were identified correctly while fewer water pixels were incorrectly assigned.

TABLE IV
TEST SET 1: PERFORMANCE ANALYSIS FOR THE BEAUFORT IMAGE

GLCP	METRICS	WGLCP
0.73	**Overall Accuracy**	0.79
0.27	**Overall Error**	0.21
0.99	**Ice: Producer's Accuracy**	0.99
0.68	**Ice: User's Accuracy**	0.74
0.36	**Water: Producer's Accuracy**	0.51
0.99	**Water: User's Accuracy**	0.99
0.46	**Kappa Statistic**	0.54

E. Texture Boundary Discrimination

An edge transect is a profile view of a GLCP or WGLCP feature as the image window moves across a row in the image. The purpose of this test is to measure and to compare the response of the GLCP and WGLCP features as they move across a texture boundary. Using the ice and water textures from the Baffin Image (Test Set 2), an artificial bipartite i
with a vertical boundary was created as shown in Figu

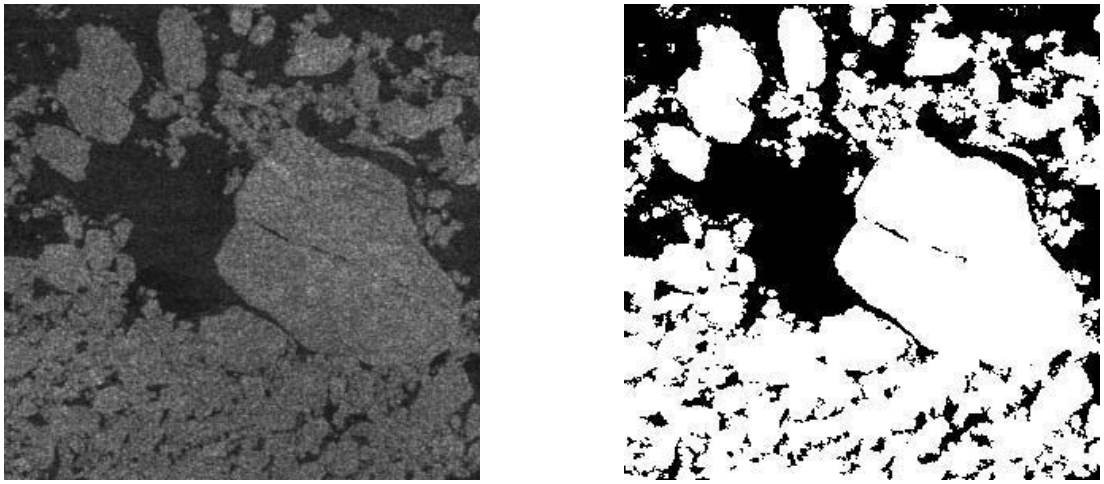

(a) Original (b) Manual Segmentation

Fig. 4. Test Set 2: SAR Sea Ice Image from Baffin Bay

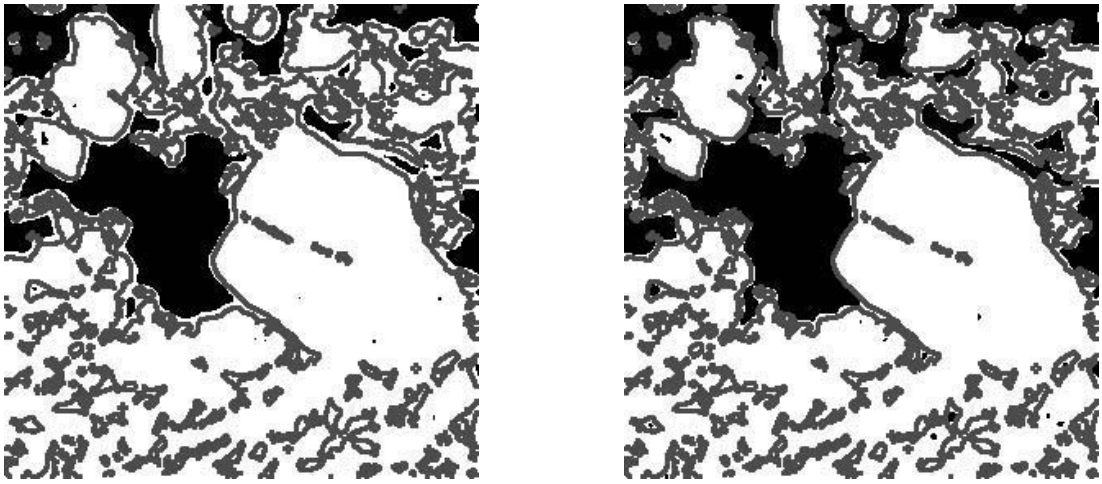

(a) Segmentation using GLCP feature set (b) Segmentation using WGLCP feature set

Fig. 5. Segmentation Results from Test Set 2: SAR Sea Ice Image from Baffin Bay

Twenty random transects were taken across the image and the GLCP and WGLCP texture features were calculated. For each texture statistic, the results for each orientation were averaged to make the features directional invariant. As well, the twenty samples were averaged to increase the signal-to-noise (SNR) ratio. The edge transect responses are displayed in Figure 7. For these results, the true boundary is indicated by a dashed vertical line.

TABLE V

TEST SET 2: PERFORMANCE ANALYSIS FOR THE BAFFIN IMAGE

GLCP	METRICS	WGLCP
0.82	**Overall Accuracy**	0.85
0.18	**Overall Error**	0.15
0.99	**Ice: Producer's Accuracy**	0.99
0.78	**Ice: User's Accuracy**	0.82
0.47	**Water: Producer's Accuracy**	0.57
0.99	**Water: User's Accuracy**	0.99
0.71	**Kappa Statistic**	0.63

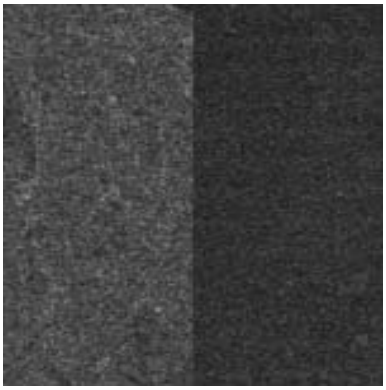

Fig. 6. Bipartite Test Image

Proceedings of the First Canadian Conference on Computer and Robot Vision (CRV'04)
0-7695-2127-4/04 $20.00 © 2004 IEEE

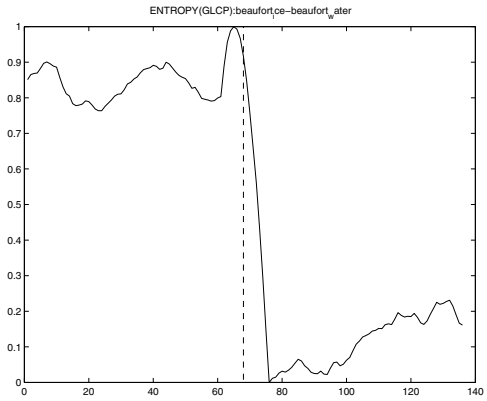

(a) GLCP: entropy results

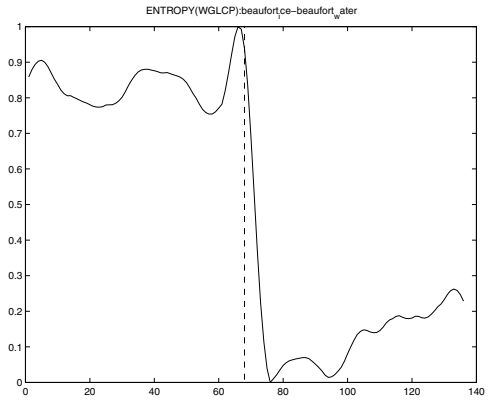

(b) WGLCP: entropy results

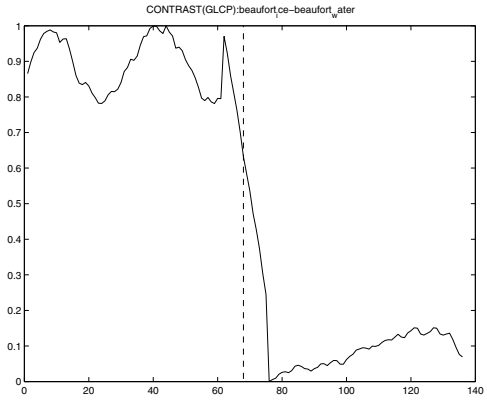

(c) GLCP: contrast results

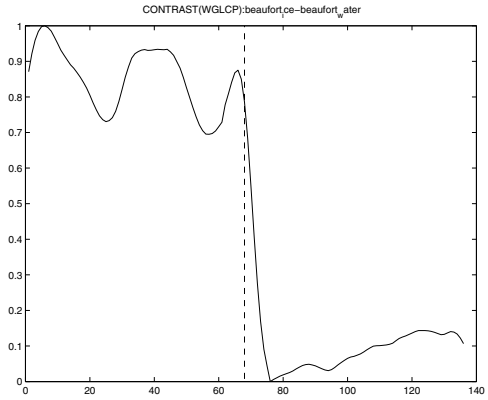

(d) WGLCP: contrast results

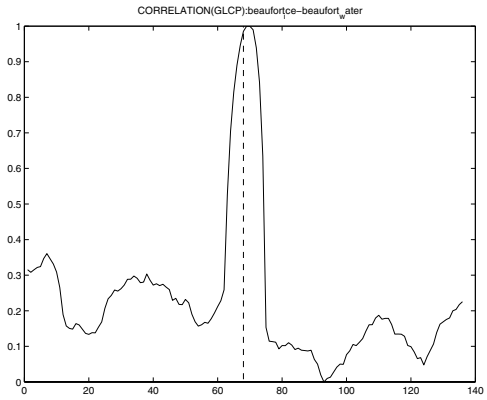

(e) GLCP: correlation results

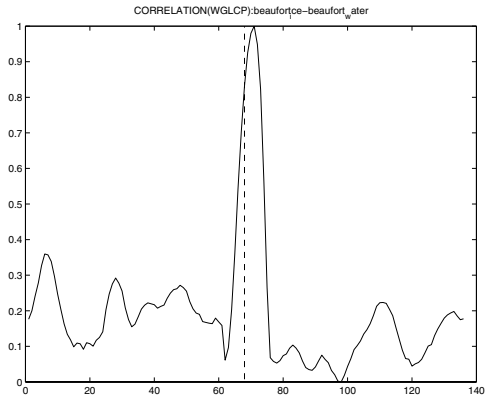

(f) WGLCP: correlation results

Fig. 7. Edge Transects

From the transect results, it is apparent that the WGLCP features have a less damped response near the boundary and thus perform better at preserving texture edges. From Table VI, it is quantitatively verified that all the WGLCP features have greater average gradients than the GLCP features. It should be noted that since the correlation statistic has an impulse-like response, the gradient was not computed.

Due to the high frequency of boundaries in SAR sea ice imagery, boundary preservation is a critical aspect for segmentation. For example, using a 15×15 window size for the image in Figure 2, 55 % of the windows contain pixels belonging to both ice and water textures. This being said, conservation of the texture boundaries has a significant impact on segmentation.

TABLE VI

AVERAGE GRADIENT RESPONSE OF THE TEXTURE BOUNDARY FOR SELECTED FEATURE STATISTICS

GLCP Gradient	Feature Statistics	WGLCP Gradient
-0.103	**Entropy**	-0.120
-0.058	**Contrast**	-0.112

The correlation statistic produces a impulse-like re

Proceedings of the First Canadian Conference on Computer and Robot Vision (CRV'04)
0-7695-2127-4/04 $20.00 © 2004 IEEE

near the SAR ice-water texture boundary. The impulse is caused from a change in contrast across the boundary. The result of this characteristic can cause confusion during segmentation; instead of segmenting ice-water, the algorithm will separate boundary versus non-boundary.

F. Computational Comparisons

Recently, there have been advances in the calculation of co-occurring texture features. Historically, the GLCPs were stored in the GLCMs which are an inefficient and slow method of calculation due to the sparse nature of co-occurring grey level pairs. As discussed in Section II, the GLCLL (Clausi & Jernigan 1998) and GLCHS (Clausi & Zhao 2002) have decreased computational time significantly from the GLCM approach. Currently, the GLCM is needed to store the weighted co-occurring probabilities. As well, an increase in computational time occurs from the need to determine the Euclidean distance of a pixel pair to the center of the image window. Therefore, a drawback of using the WGLCP texture statistics is that there is a significant increase in computational time needed.

More investigation is necessary to determine if the computation time required for calculating the WGLCP features can be decreased.

V. Conclusion

Texture discrimination is a significant aspect in segmenting remote sensing imagery. Texture features from GLCPs are very popular and well accepted amongst remote sensing communities. Albeit an innovative technique, GLCP features have a predisposition to misclassify and erode texture boundaries due to the large window sizes needed to capture meaningful statistics.

We formulated a set of Gaussian weighted co-occurring features which proved to be better at discriminating texture boundaries and image segmentation. Through the test sets, there was a notable improvement in segmentation. We also showed that the edge response of the WGLCP is sharper, thus preserving texture boundaries compared to the GLCP features. Currently, a drawback in using WGLCP features is that a significant increase in computational time is required. More investigation is necessary to try reducing the computational speed of calculating the WGLCP features.

Acknowledgments

The authors would like to thank the members of the SIP (Signal and Image Processing) group at the University of Waterloo for their support. As well, thanks are extended to Priyesh Shukla for his expertise in the manual segmentation of the test data and creating figures. Special thanks to the Canadian Ice Services (CIS) for providing the data sets and to GEOIDE (Geomatics for Informed Decisions), `http:www.geoide.ulaval.ca.` for funding of this project.

References

Baraldi, A. & Parmiggiani, F. (1995), 'An investigation of the textural characteristics associated with gray level cooccurrence matrix statistical parameters', *IEEE Trans. Geosci. Remote Sensing* **33**(2), 293–303.

Barber, D. G. & LeDrew, E. F. (1991), 'SAR sea ice discrimination using texture statistics: a multivariate approach', *Photgrammetric Engineering Engineering and Remote Sensing* **57**(4), 385–395.

Barber, D. G., Shokr, M. E., Fernandes, R. A., Soulis, E. D. & Flett, D. G. (1993), 'A comparison of second-order classifiers for SAR sea ice discrimination', *Photogrammetric Engineering and Remote Sensing* **59**(9), 1397–1408.

Brodatz, P. (1966), 'Textures: A photographic album for artists and designers', *Dover* .

Clausi, D. A. (1996), 'Texture segmentation of SAR sea ice imagery', *University of Waterloo, phD Thesis* .

Clausi, D. A. (2002), 'An analysis of co-occurrence texture statistics as a function of grey level quantization', *Can. J. Remote Sensing* **28**(1), 45–62.

Clausi, D. A. & Jernigan, M. E. (1998), 'A fast method to determine co-occurrence texture features', *IEEE Trans. Geosci. Remote Sensing* **36**(1), 298–300.

Clausi, D. A. & Yue, B. (2003), 'Comparing cooccurrence probabilities and markov random fields for texture analysis of SAR sea ice imagery', *IEEE Trans. Geosci. Remote Sensing* . (Accepted for future publication).

Clausi, D. A. & Zhao, Y. (2002), 'Rapid extraction of image texture by co-occurrence using a hybrid data structure', *Computers and Geosciences* **28**, 763–774.

Haralick, R. M., Shanmugam, K. & Dinstein, I. (1973), 'Textural features for image classification', *IEEE Trans. Sys. Man Cyber.* **3**(6), 610–621.

Holmes, Q. A., Nuesch, D. R. & Shuchman, R. A. (1984), 'Texture analysis and real-time classification of sea-ice types using digital SAR data', *IEEE Trans. Geosci. Remote Sensing* **22**(2), 113–120.

Shokr, M. E. (1991), 'Evaluation of second-order texture parameters for sea ice classification from radar images', *J. Geophysical Research* **96**(C6), 625–640.

Soh, L. K. & Tsatsoulis, C. (1999), 'Texture analysis of SAR sea ice imagery using gray level co-occurence matrices', *IEEE Trans. Geosci. Remote Sensing* **37**(2), 780–794.

Tuceryan, M. & Jain, A. K. (1993), *Handbook of Pattern Recognition and Computer Vision, Chapter 2: Texture Analysis*, Singapore: World Scientific.